



Machine Learning based tool for CMS RPC currents quality monitoring

E. Shumka^{6,*}, A. Samalan¹, M. Tytgat¹, M. El Sawy², G.A. Alves³, F. Marujo³, E.A. Coelho³, E.M. Da Costa⁴, H. Nogima⁴, A. Santoro⁴, S. Fonseca De Souza⁴, D. De Jesus Damiao⁴, M. Thiel⁴, K. Mota Amarilo⁴, M. Barroso Ferreira Filho⁴, A. Aleksandrov⁵, R. Hadjiiska⁵, P. Iaydjiev⁵, M. Rodozov⁵, M. Shopova⁵, G. Soultanov⁵, A. Dimitrov⁶, L. Litov⁶, B. Pavlov⁶, P. Petkov⁶, A. Petrov⁶, S.J. Qian⁷, H. Kou^{8,9}, Z.-A. Liu^{8,9}, J. Zhao^{8,9}, J. Song^{8,9}, Q. Hou^{8,9}, W. Diao^{8,9}, P. Cao^{8,9}, C. Avila¹⁰, D. Barbosa¹⁰, A. Cabrera¹⁰, A. Florez¹⁰, J. Fraga¹⁰, J. Reyes¹⁰, Y. Assran^{11,12}, M.A. Mahmoud¹³, Y. Mohammed¹³, I. Crotty¹³, I. Laktineh¹⁵, G. Grenier¹⁵, M. Gouzevitch¹⁵, L. Mirabito¹⁵, K. Shchablo¹⁵, I. Bagaturia¹⁶, I. Lomidze¹⁶, Z. Tsamalaidze¹⁶, V. Amoozegar¹⁷, B. Boghrati^{17,18}, M. Ebraimi¹⁷, M. Mohammadi Najafabadi¹⁷, E. Zareian¹⁷, M. Abbrescia¹⁹, G. Iaselli¹⁹, G. Pugliese¹⁹, F. Loddo¹⁹, N. De Filippis¹⁹, R. Aly^{19,36}, D. Ramos¹⁹, W. Elmetenawee¹⁹, S. Leszki¹⁹, I. Margjeka¹⁹, D. Paesani¹⁹, L. Benussi²⁰, S. Bianco²⁰, D. Piccolo²⁰, S. Meola²⁰, S. Buontempo²¹, F. Carnevali²¹, L. Lista²¹, P. Paolucci²¹, F. Fienga²², A. Braghieri²³, P. Salvini²³, P. Montagna²⁴, C. Riccardi²⁴, P. Vitulo²⁴, E. Asilar²⁵, J. Choi²⁵, T.J. Kim²⁵, S.Y. Choi²⁶, B. Hong²⁶, K.S. Lee²⁶, H.Y. Oh²⁶, J. Goh²⁷, I. Yu²⁸, C. Uribe Estrada²⁹, I. Pedraza²⁹, H. Castilla-Valdez³⁰, A. Sanchez-Hernandez³⁰, R.L. Fernandez³⁰, M. Ramirez-Garcia³¹, E. Vazquez³¹, M.A. Shah³¹, N. Zaganidis³¹, A. Radi^{32,14}, H. Hoorani³³, S. Muhammad³³, A. Ahmad³³, I. Asghar³³, W.A. Khan³³, J. Eysermans³⁴, F. Torres Da Silva De Araujo³⁵, on behalf of the CMS Muon Group

¹ Ghent University, Department of Physics and Astronomy, Proeftuinstraat 86, B-9000 Ghent, Belgium

² Université Libre de Bruxelles, Avenue Franklin Roosevelt 50-1050 Bruxelles, Belgium

³ Centro Brasileiro Pesquisas Físicas, R. Dr. Xavier Sigaud, 150 - Urca, Rio de Janeiro - RJ, 22290-180, Brazil

⁴ Dep. de Física Nuclear e Altas Energias, Instituto de Física, Universidade do Estado do Rio de Janeiro, Rua Sao Francisco Xavier, 524, BR - Rio de Janeiro 20559-900, RJ, Brazil

⁵ Bulgarian Academy of Sciences, Inst. for Nucl. Res. and Nucl. Energy, Tzarigradsko shaussee Boulevard 72, BG-1784 Sofia, Bulgaria

⁶ Faculty of Physics, University of Sofia, 5 James Bourchier Boulevard, BG-1164 Sofia, Bulgaria

⁷ School of Physics, Peking University, Beijing 100871, China

⁸ State Key Laboratory of Particle Detection and Electronics, Institute of High Energy Physics, Chinese Academy of Sciences, Beijing 100049, China

⁹ University of Chinese Academy of Sciences, No.19(A) Yuquan Road, Shijingshan District, Beijing 100049, China

¹⁰ Universidad de Los Andes, Carrera 1, no. 18A - 12, Bogotá, Colombia

¹¹ Egyptian Network for High Energy Physics, Academy of Scientific Research and Technology, 101 Kasr El-Einy St., Cairo, Egypt

¹² Suez University, Elsalam City, Suez - Cairo Road, Suez 43522, Egypt

¹³ Center for High Energy Physics(CHEP-FU), Faculty of Science, Fayoum University, 63514 El-Fayoum, Egypt

¹⁴ Department of Physics, Faculty of Science, Ain Shams University, Cairo, Egypt

¹⁵ Univ Lyon, Univ Claude Bernard Lyon 1, CNRS/IN2P3, IP2I Lyon, UMR 5822, F-69622, Villeurbanne, France

¹⁶ Georgian Technical University, 77 Kostava Str., Tbilisi 0175, Georgia

¹⁷ School of Particles and Accelerators, Institute for Research in Fundamental Sciences (IPM), P.O. Box 19395-5531, Tehran, Iran

¹⁸ School of Engineering, Damghan University, Damghan, 3671641167, Iran

¹⁹ INFN, Sezione di Bari, Via Orabona 4, IT-70126 Bari, Italy

²⁰ INFN, Laboratori Nazionali di Frascati (LNF), Via Enrico Fermi 40, IT-00044 Frascati, Italy

²¹ INFN, Sezione di Napoli, Complesso Univ. Monte S. Angelo, Via Cintia, IT-80126 Napoli, Italy

²² Dipartimento di Ingegneria Elettrica e delle Tecnologie dell'Informazione - Università Degli Studi di Napoli Federico II, IT-80126 Napoli, Italy

²³ INFN, Sezione di Pavia, Via Bassi 6, IT-Pavia, Italy

²⁴ INFN, Sezione di Pavia and University of Pavia, Via Bassi 6, IT-Pavia, Italy

²⁵ Hanyang University, 222 Wangsimni-ro, Sageun-dong, Seongdong-gu, Seoul, Republic of Korea

²⁶ Korea University, Department of Physics, 145 Anam-ro, Seongbuk-gu, Seoul 02841, Republic of Korea

* Corresponding author.

E-mail address: elton.shumka@cern.ch (E. Shumka).

<https://doi.org/10.1016/j.nima.2023.168449>

Received 21 November 2022; Received in revised form 28 February 2023; Accepted 20 April 2023

Available online 15 June 2023

0168-9002/© 2023 The Author(s). Published by Elsevier B.V. This is an open access article under the CC BY-NC license (<http://creativecommons.org/licenses/by-nc/4.0/>).

²⁷ Kyung Hee University, 26 Kyungheedaero, Dongdaemun-gu, Seoul 02447, Republic of Korea

²⁸ Sungkyunkwan University, 2066 Seobu-ro, Jangan-gu, Suwon, Gyeonggi-do 16419, Republic of Korea

²⁹ Benemerita Universidad Autonoma de Puebla, Puebla, Mexico

³⁰ Cinvestav, Av. Instituto Politécnico Nacional No. 2508, Colonia San Pedro Zacatenco, CP 07360, Ciudad de Mexico D.F., Mexico

³¹ Universidad Iberoamericana, Mexico City, Mexico

³² Sultan Qaboos University, Al Khoudh, Muscat 123, Oman

³³ National Centre for Physics, Quaid-i-Azam University, Islamabad, Pakistan

³⁴ Massachusetts Institute of Technology, 77 Massachusetts Ave, Cambridge, MA 02139, United States

³⁵ III. Physikalisches Institut (A), RWTH Aachen University, Sommerfeldstrasse D-52056, Aachen, Germany

³⁶ Physics Department, Faculty of Science, Helwan University, Ain Helwan 11795, Cairo, Egypt

ARTICLE INFO

Keywords:

CMS experiment
Resistive Plate Chambers
Machine Learning
Gas detectors
Monitoring tools

ABSTRACT

The muon system of the CERN Compact Muon Solenoid (CMS) experiment includes more than a thousand Resistive Plate Chambers (RPC). They are gaseous detectors operated in the hostile environment of the CMS underground cavern on the Large Hadron Collider where pp luminosities of up to $2 \times 10^{34} \text{ cm}^{-2}\text{s}^{-1}$ are routinely achieved. The CMS RPC system performance is constantly monitored and the detector is regularly maintained to ensure stable operation. The main monitorable characteristics are dark current, efficiency for muon detection, noise rate etc. Herein we describe an automated tool for CMS RPC current monitoring which uses Machine Learning techniques. We further elaborate on the dedicated generalized linear model proposed already and add autoencoder models for self-consistent predictions as well as hybrid models to allow for RPC current predictions in a distant future.

1. Introduction

The muon system of the CMS experiment [1] includes 1056 Resistive Plate Chambers (RPC) operated at nominal high voltages (HV) of 9–10 kV. Monitoring their dark current evolution, spotting deviations from normal performance and anticipating an HV failure that would immediately propagate to higher detector control levels is an unfeasible task for an online operator. Detector parameters are abundant [2], thus HV problems manifest differently, making the human intervention inefficient. Therefore, an automated process with built-in notification logic and mechanism is highly sought after for development and further implementation. Being able to spot increasing current tendencies, for example, before they lead to an error is very important for controlling detector operation. An automated tool that performs anomaly detection for the RPC currents by using Machine Learning (ML) methods is presented here.

Two types of ML approaches are used: Generalized Linear Models (GLM) and Autoencoders.

In the GLM case, a set of parameters such as environmental conditions, LHC parameters and detector working points are used to characterize the behavior of the current.

In the autoencoder case, the full set of the RPC HV system currents is used as an input and the autoencoder network is trained to reproduce these inputs onto the output neurons.

Both approaches show very good predictive capabilities that are the basis for the monitoring tool. All the developed tools are integrated in a framework that can be easily accessed and controlled by a specially developed Web User Interface that allows the end-users to work with the monitoring tool in a simple manner. It is being deployed for use during the CERN LHC Run-3 data-taking period.

2. Generalized linear model

The GLM depicted in Fig. 1 is a generalization of a simple linear regression used to model the current as a function of the following sets of parameters:

- Environmental conditions: temperature (T), relative humidity (RH) and pressure (P)
- LHC parameters: instantaneous luminosity (L) and integrated luminosity ($\sum L$)
- Applied HV

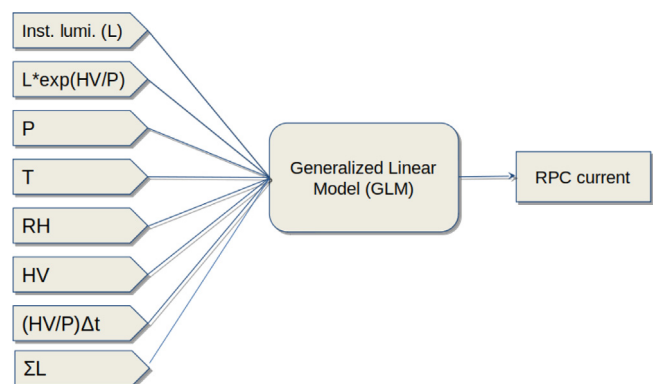


Fig. 1. The structure of the GLM.

- Combined terms: $L \times \exp(HV/P)$ and $(\sum HV/P)\Delta t$, where Δt is the length of the time period with no luminosity

The $\sum L$ term replaces the Δt term used in the initially proposed model [3]. The improvement is inspired by [4]. The first combined term is to account for the exponential increase of gas multiplication with the raising of HV while the second one is to account for the chamber relaxation and the drop of the current baseline during cosmic data taking, when there is no beam luminosity and the chambers are at their working point. All the remaining terms and the motivation for including them are discussed in [3].

3. Autoencoder

In contrast to the GLM approach, where we use detailed knowledge for the physical processes taking place in a particular type of detector in order to build the ML model, in this section we take a more general approach, namely develop an ML model based on cross-correlation between different detector modules, thus applicable for detector systems consisting of a large number of RPC chambers. We develop an ML algorithm based on an autoencoder model. Autoencoders are neural networks that are trained to encode the input into a number of neurons that is lower than the number of inputs themselves and then decode that same information onto the output layer (Fig. 2). During the learning stage, the autoencoder is supposed to learn the collective behavior of all the RPC chambers. Such an autoencoder could be used

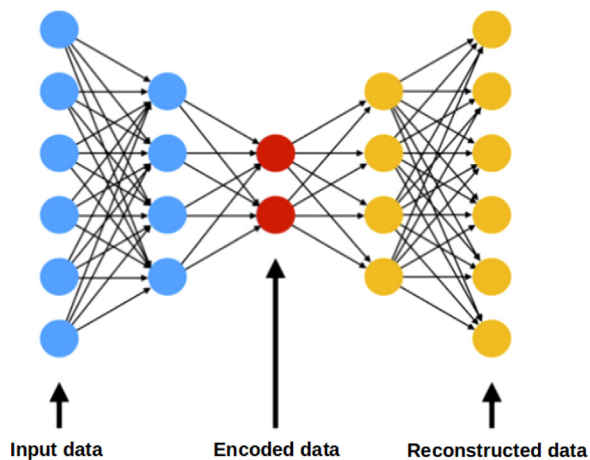


Fig. 2. Topology of an autoencoder.

later on to spot an anomalous behavior of a single or a small subset of RPC chambers.

In this work, the set of RPC currents at a given moment in time is given as an input to the autoencoder and the network is trained to reproduce them on its output layer. The number of input and output neurons is 773, which corresponds to the number of HV channels in the RPC system. The hidden layers count respectively: 512, 128, 64, 128 and 512 neurons.

4. Hybrid network

As discussed above, GLM describes individual RPC chamber behavior while the autoencoder describes collective correlations of the whole system. In order to use their best qualities, we combine the two approaches into a model, referred to as a hybrid network. In this model, a set of GLM equal in size to the number of HV channels provide as output the currents for a given moment in time. These currents are then used as inputs for an autoencoder, as shown in Fig. 3. The hybrid network is tested in a distant prediction scenario, where the end of the training period is separated in time (e.g. 1 year) from the beginning of the prediction period. Its performance in such a scenario (Section 7) shows that it can be used as indication for current values that we could expect on a system level for some specified conditions (e.g. the luminosity of the High-Luminosity LHC).

5. Monitoring tool

The accurate predictions of the currents performed by both the GLM and autoencoder can be used to detect anomalies in the RPC detector current performance. The implemented tool follows the workflow presented in the flowchart in Fig. 4. Raw data coming from the

CMS non-physics event bus, referred to as online condition data, are written in the cms_omds_adg database copy. For each point in time for which data is available, the tool performs comparisons between the measured and predicted RPC currents. If differences higher than some predetermined threshold values are detected for a given HV channel, a flag is raised and the case of that particular channel is followed. There are two thresholds, the lower one inducing a warning and the higher one inducing an error. After a specified number of points in time, the running average of the differences is calculated and if this average exceeds the thresholds, a warning or an error is sent to the end-users. This allows for the detection of problematic HV channels before they result in an HV channel trip.

6. Software implementation

The monitoring tool is programmed in Python. Tensorflow [5] is used for the implementation of ML. The software is conceptualized and implemented with modularity in mind (Fig. 5). All modules communicate back-and-forth with a database. The “Trainer Module” reads the training data from a table and after performing the training, writes back the ML model parameters in another database table. The “Estimator Module” loads the models and performs predictions, which are also stored into the database. Finally, the “Notifications Manager” searches for anomalies in the current values, as described in the previous section and provides notifications.

7. Performance results

ML model performance validation is done for three different training scenarios:

- Short-term training (ST), with data from May to September 2018. Such models are able to spot a rapid increase in the RPC currents.
- Mid-term training (MT), with data from July 2017 to July 2018, appropriate for describing the seasonal behavior of the currents.
- Long-term training (LT), with data from May 2016 to July 2018, appropriate for modeling the overall RPC currents evolution.

All models are tested against the RPC currents measured in the two-month period between September and October of 2018. These tests show that GLM performs best in LT scenario (Fig. 6), while the autoencoder performs best in ST (Fig. 7). The hybrid network performance is shown in Fig. 8. The Mean Absolute Error (MAE) and Mean Squared Error (MSE), which are used as performance metrics, are defined as:

$$\text{MAE} = \sum_{i=1}^N \frac{|I_{mon}^i - I_{pred}^i|}{N} \quad (1)$$

$$\text{MSE} = \sum_{i=1}^N \frac{(I_{mon}^i - I_{pred}^i)^2}{N} \quad (2)$$

The sigma of the histogram in both cases is $<1 \mu\text{A}$, which shows that both models have excellent predictive capabilities consistent with the

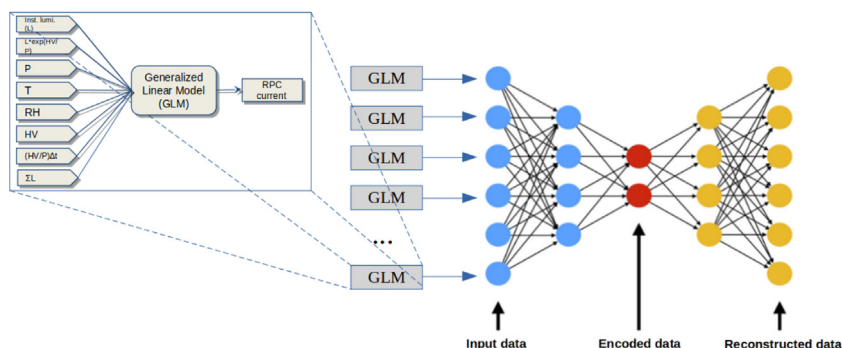


Fig. 3. The hybrid network (the left and right parts of this figure are the same as Figs. 1 and 2, respectively).

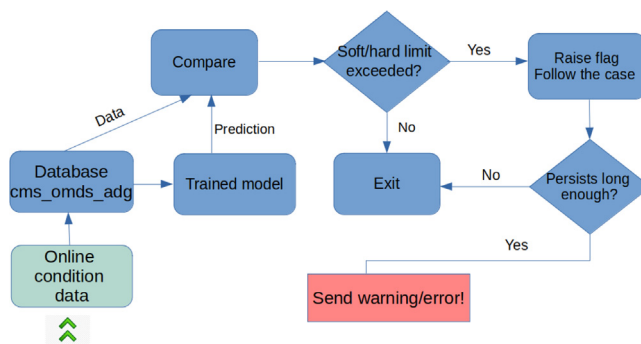


Fig. 4. Monitoring tool workflow.

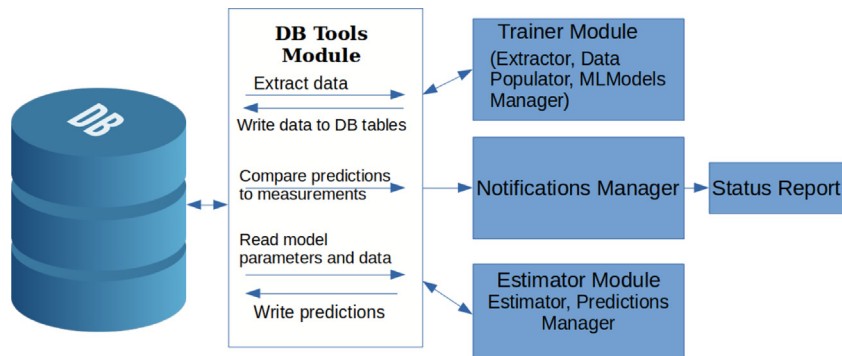


Fig. 5. Software structure.

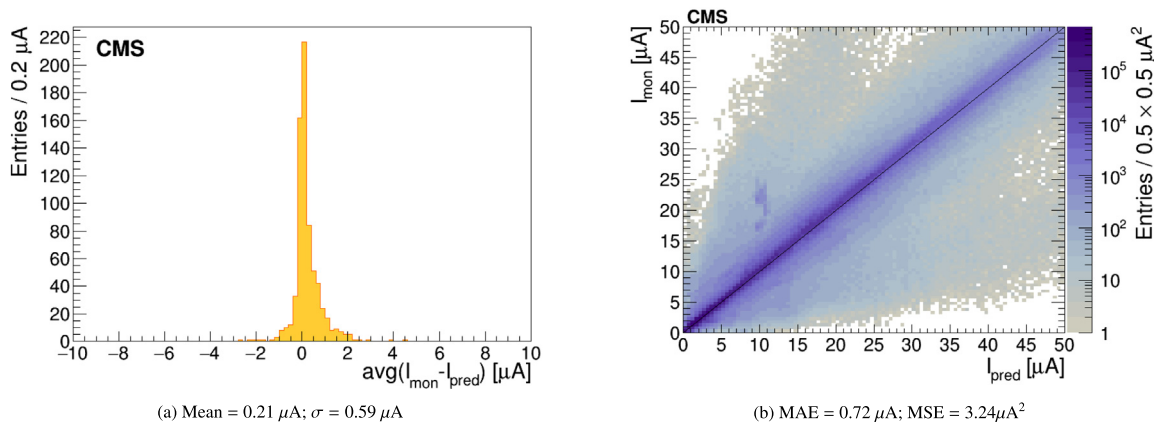


Fig. 6. GLM LT performance.

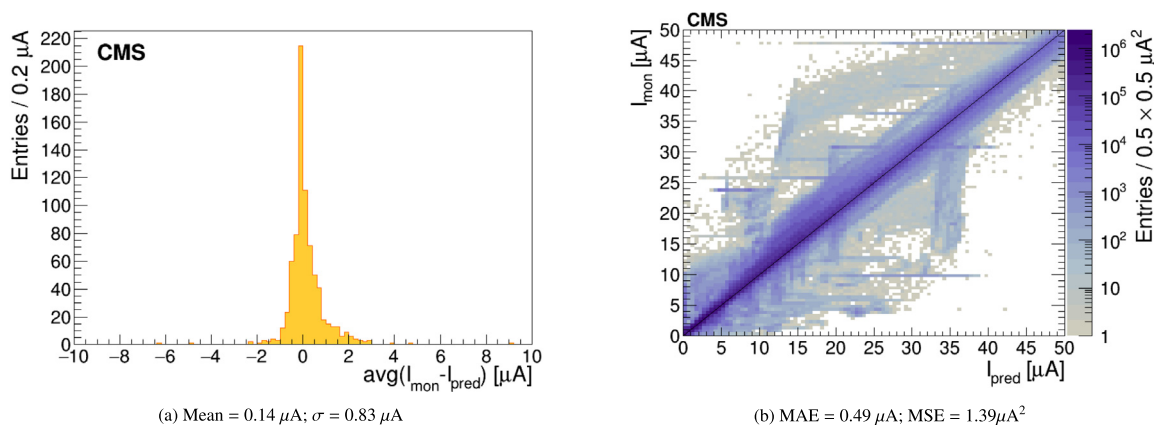


Fig. 7. Autoencoder ST performance.

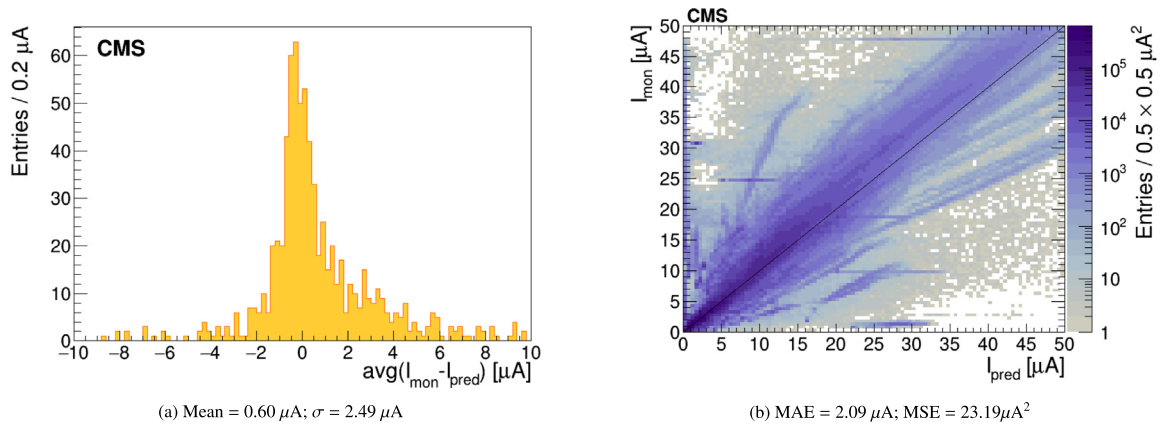


Fig. 8. Hybrid network performance.

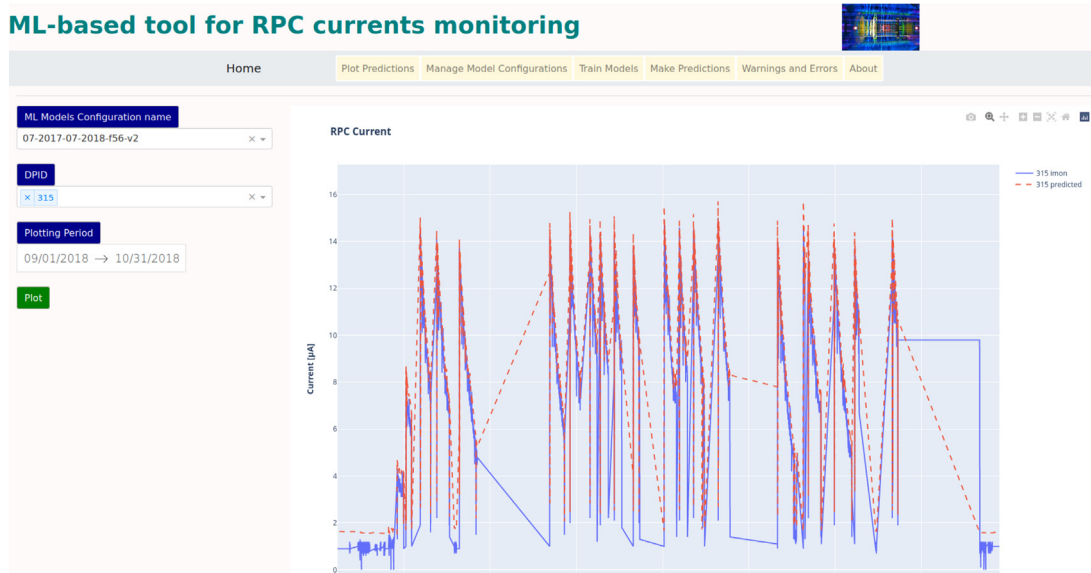


Fig. 9. Screenshot of the Web User Interface.

Table 1

Performance results.

Model class	Training period	Prediction period	1D histo mean [μA]	1D histo sigma [μA]	2D histo MAE [μA]	2D histo MSE [μA^2]
GLMv2	18-05-01 to 18-09-01	18-09-01 to 18-10-30	-0.02	1.65	1.23	7.62
GLMv2	17-07-01 to 18-07-01	18-09-01 to 18-10-30	0.33	1.66	1.23	7.42
GLMv2	16-05-01 to 18-07-01	18-09-01 to 18-10-30	0.21	0.59	0.72	3.24
Autoencoder	18-05-01 to 18-09-01	18-09-01 to 18-10-30	0.14	0.83	0.49	1.39
Autoencoder	17-07-01 to 18-07-01	18-09-01 to 18-10-30	0.69	1.44	0.96	4.18
Autoencoder	16-05-01 to 18-07-01	18-09-01 to 18-10-30	0.42	1.40	0.85	3.16
GLMv2	16-05-01 to 17-07-01	18-09-01 to 18-09-30	-0.24	2.59	1.92	18.69
Autoencoder	16-05-01 to 17-07-01	18-09-01 to 18-09-30	0.06	2.51	2.14	22.57
Hybrid	16-05-01 to 17-07-01	18-09-01 to 18-09-30	0.60	2.49	2.09	23.19

uncertainty in the current measurement which is also of that same order. All performance results are shown in Table 1.

Fig. 10 shows the case of an RPC chamber where the predicted current increasingly diverges from the measured one. It was found that this discrepancy could be explained with the appearance of a gas leak in this chamber around the same time.

8. Deployment on the CERN PaaS platform

The monitoring tool is accessible through a Web User Interface that is being deployed on the CERN Platform-as-a-Service (PaaS) virtual

environment (Fig. 9). It is based on OpenShift [6], a platform which allows for containerized application deployment.

9. Conclusions

We use Machine Learning (ML) methods for anomaly detection in the current behavior of CMS Resistive Plate Chambers. The excellent accuracy of the ML model predictions allow us to implement a powerful monitoring tool which notifies the end-users about potential high-voltage channel deviations from normal behavior and increased risk of operational failures. The monitoring tool has been developed and

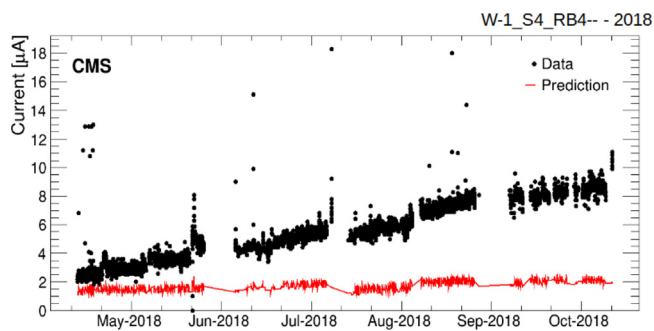


Fig. 10. Monitored and predicted currents for an RPC chamber in W-1 of the CMS barrel.

will be fully deployed for use during the Year-End Technical Stop (YETS22/23).

Declaration of competing interest

The authors declare that they have no known competing financial interests or personal relationships that could have appeared to influence the work reported in this paper.

Acknowledgments

We congratulate our colleagues in the CERN accelerator departments for the excellent performance of the LHC and thank the technical

and administrative staffs at CERN and at other CMS institutes for their contributions to the success of the CMS effort. In addition, we gratefully acknowledge the computing centers and personnel of the Worldwide LHC Computing Grid and other centers for delivering so effectively the computing infrastructure essential to our analyses. Finally, we acknowledge the enduring support for the construction and operation of the LHC, the CMS detector, and the supporting computing infrastructure provided by the following funding agencies: FWO (Belgium); CNPq, CAPES and FAPERJ (Brazil); MES and BNSF (Bulgaria); CERN; CAS, MoST, and NSFC (China); Minciencias (Colombia); CEA and CNRS/IN2P3 (France); SRNSFG (Georgia); DAE and DST (India); IPM (Iran); INFN (Italy); MSIP and NRF (Republic of Korea); BUAP, CINVESTAV, CONACYT, LNS, SEP, and UASLP-FAI (Mexico); PAEC (Pakistan); DOE and NSF (USA).

References

- [1] CMS Collaboration, The CMS experiment at the CERN LHC, *J. Instrum.* 3 (2008) S08004, URL <https://doi.org/10.1088/1748-0221/3/08/S08004>.
- [2] CMS Collaboration, Performance of the CMS muon detector and muon reconstruction with proton-proton collisions at $\sqrt{s} = 13$ TeV, *J. Instrum.* 13 (2018) P06015, URL <https://doi.org/10.48550/arXiv.1804.04528>.
- [3] A. Samalan, et al., A new approach for CMS RPC currents monitoring using machine learning techniques, *J. Instrum.* 15 (2020) C10009, URL <http://dx.doi.org/10.1088/1748-0221/15/10/C10009>.
- [4] A. Gelmi, R. Guida, B. Mandelli, on behalf of the CMS Muon Group, Gas mixture quality studies for the CMS RPC detectors during LHC run 2, *J. Instrum.* 16 (2021) C04004, URL <http://dx.doi.org/10.1088/1748-0221/16/04/C04004>.
- [5] Tensorflow, 2022, URL <https://www.tensorflow.org/>.
- [6] Red Hat, OpenShift documentation, 2022, URL <https://docs.openshift.com/>.